AJNR

Fragile X Premutation Carriers: Characteristic MR Imaging Findings of Adult Male Patients with Progressive Cerebellar and Cognitive Dysfunction

James A. Brunberg, Sebastien Jacquemont, Randi J. Hagerman, Elizabeth M. Berry-Kravis, Jim Grigsby, Maureen A. Leehey, Flora Tassone, W. Ted Brown, Claudia M. Greco and Paul J. Hagerman

AJNR Am J Neuroradiol 2002, 23 (10) 1757-1766
http://www.ajnr.org/content/23/10/1757

AJNR Am J Neuroradiol 23:1757–1766, November/December 2002

Fragile X Premutation Carriers: Characteristic MR Imaging Findings of Adult Male Patients with Progressive Cerebellar and Cognitive Dysfunction

James A. Brunberg, Sebastien Jacquemont, Randi J. Hagerman Elizabeth M. Berry-Kravis, Jim Grigsby, Maureen A. Leehey, Flora Tassone, W. Ted Brown, Claudia M. Greco, and Paul J. Hagerman

BACKGROUND AND PURPOSE: **Our purpose was to characterize the findings of MR imaging of the brain of adult male fragile X premutation carriers with a recently identified disorder characterized by ataxia, tremor, rigidity, and cognitive dysfunction.**

METHODS: **MR imaging studies of the brain of 17 male patients were characterized for signal intensity and for size of ventricles, cerebral and cerebellar sulci, and brain stem. Comparison was made with age- and sex-matched control participants. Southern blot and/or polymerase chain reaction methods were used to analyze CGG trinucleotide repeats in the fragile X mental retardation 1 gene.**

RESULTS: **Fifteen of 17 patients showed symmetrically decreased T1 and increased T2 signal intensity in cerebellar white matter lateral, superior, and inferior to the dentate nuclei. Fourteen of 17 had similar signal intensity alterations in the middle cerebellar peduncles. Cerebellar cortical atrophy was present in 16 of 17 and cerebral atrophy in 17 of 17. Evan's Index as a measure of ventricular size averaged 0.35 (range, 0.25–0.46), with that for age-matched control participants averaging 0.28 (range, 0.24–0.31) ($P < .005$). The mean third ventricle width was 11 mm (for control participants, 6 mm; $P < .01$). Corpus callosum was thinned in 14 of 16 participants. Middle cerebellar peduncles were atrophic when compared with those of control participants ($P < .005$). Pontine transverse dimension was 25 mm (for control participants, 31 mm; $P < .005$), and rostral-caudal length averaged 26 mm (for control participants, 29 mm; $P < .005$). CGG repeats clustered in the low to mid premutation range (86 ± 10 CGG repeats) in the 17 patients.**

CONCLUSION: **MR imaging findings in symptomatic male fragile X premutation carriers are characteristic of this disorder. Recognition of these alterations may support a specific diagnosis and may have implications for the potential occurrence of fragile X syndrome in the children of reproductive age female relatives.**

Fragile X syndrome is the most common inherited form of mental retardation, with the carrier frequency in the general population being approximately one in 250 female and one in 760 male persons (1, 2). The disorder is caused by an expansion in excess of 200 repeats (full mutation expansion) of a trinucleotide element, $(CGG)_n$, located in the 5′ untranslated region of the fragile X mental retardation 1 (*FMR1*) gene (3). Full mutation expansions are generally accompanied by silencing of the *FMR1* gene, with attendant lack of *FMR1* protein (FMRP) synthesis; it is the lack of FMRP that leads to fragile X syndrome. Trinucleotide expansions that are in the 55- to 200-repeat range are termed *premutations*. Normal persons may have a range of approximately five to 54 repeats. Carriers of premutations typically have normal intelligence quotients, although emotional difficulties and subtle physical features occur in approximately 25% (4–8). A unique clinical finding in female

Received March 20, 2002; accepted after revision July 11.

From the Departments of Radiology (J.A.B.) and Biological Chemistry (F.T., P.J.H), University of California, Davis, School of Medicine, CA; the M.I.N.D. Institute (S.J., R.J.H.) and the Departments of Pediatrics (R.J.H.) and Pathology (C.M.G.), University of California Davis Medical Center, Sacramento, CA; the Department of Pediatrics (E.M.B.-K.), Rush Presbyterian Hospital, Chicago, IL; the Departments of Medicine (J.G.) and Neurology (M.A.L.), University of Colorado Health Sciences Center, Denver, CO; and the Department of Human Genetics (W.T.B.), New York State Institute for Basic Research in Developmental Disabilities, Staten Island, NY.

Address reprint requests to James A. Brunberg, MD, MHSA, Department of Radiology, University of California, Davis, 4860 Y Street, Suite 3100, Sacramento, CA 95817.

patients with the premutation (ie, a feature not seen in women with the full mutation expansion) is premature ovarian failure, which is present in approximately 20% of female carriers of premutation expansions (9, 10). The standard model for fragile X syndrome does not predict this form of clinical involvement.

A separate and unique form of clinical involvement has recently been reported in a subgroup of older male carriers of the fragile X premutation (11). Among these male carriers, all older than 50 years, progressive intention tremor and ataxia have developed. These symptoms are accompanied by progressive cognitive and behavioral difficulties, including memory loss, executive function deficits, anxiety, and reclusive behavior. More significant dementia has been observed to occur in a limited number of patients (11). In four cases studied to date, neuropathologic examination revealed eosinophilic intranuclear inclusion in neurons and astrocytes (12). These inclusions are found throughout the cortex and brain stem, with the greatest diffusion in the hippocampus. Purkinje cells did not possess these inclusions, although there was evidence of axonal degeneration in the cerebellum in one of four cases (12, 13). The cerebellum has also displayed spongiform changes in the deep cerebellar white matter. Our purpose was to describe the imaging findings of 17 male patients with fragile X premutation with varying clinical combinations of tremor, ataxia, rigidity, and cognitive decline. Clinical and preliminary imaging findings of four of these patients have been published (11).

TABLE 1: Clinical, neuropsychologic, and molecular data from 17 patients

	Mean or %	SD	No. of Patients
Age at MR imaging	68 years	5.5	17
Age at tremor onset	58.3 years	3.9	15
Age at ataxia onset	61.6 years	5.6	15
Significant impairment			
Writing	89%		17
Walking	50%		17
Tremor	89%		17
Character of tremor			
Kinetic > postural	100%		15
Discrete resting tremor	58%		15
Gait ataxia	89%		17
Dyssynergia	72%		17
Tone, mild increase	47%		14
Neuropsychologic data			
VIQ	98	16	6
PIQ	83	17	6
FSIQ	91	18	6
Executive function deficits	100%		6
VIQ < 85	33%		6
PIQ < 85	66%		6
Impotence	100%		6
CGG repeat	86	10	17
FMRP level	77.5%*	9%	6
mRNA level	2.53-fold†	0.48	6

* Percentage of lymphocytes that are positive for fragile X mental retardation 1 protein immuno-cytochemical staining for fragile X mental retardation 1 protein (19, 46).

† 2.53-fold increase over normal (16, 46).

Note.—VIQ indicates verbal intelligence quotient; PIQ, performance intelligence level; FSIQ, full scale intelligence quotient; FMRP, fragile X mental retardation 1 protein; mRNA, messenger RNA.

Methods

Study Participants

Seventeen male patients with a mean age of 68 years (range, 59–77 years) were recruited through families with children affected by fragile X syndrome. The carrier male patients were all affected by a progressive cerebellar disorder, and each underwent clinical and MR imaging evaluation at one of eight medical centers. A summary of clinical symptoms, examination findings, disease course, and patient age is presented in Table 1. Fourteen normal male control participants with a mean age of 66 years (range, 56–76 years) were also included in the study.

Laboratory Evaluation

Fragile X premutation status was established by DNA analysis by using Southern blot and/or polymerase chain reaction methods as described (14, 15). Analyses of *FMR1* messenger RNA and FMRP levels were performed as described by Tassone et al (16, 19) and Willemsen et al (17, 18).

Imaging Protocol

MR imaging of the brain was performed at 1.5 T for 13 patients and at 0.3 T for four patients. Axial view T1- and T2-weighted sequences were available for all patients, and sagittal view T1-weighted images were available for 14 patients. Sagittal view T1-weighted and axial view T1- and T2-weighted images were available for the 14 normal male control participants. For all symptomatic patients and control participants, frontal, parietal, temporal, and cerebellar cortical volumes were graded as being normal or as showing mild, moderate, or severe volume loss as manifest by size of regional sulci. White matter of the frontal, parietal, and occipital lobes and white matter of the cerebellum and brain stem were graded in a similar manner for alterations in signal intensity on T1- and T2-weighted images. Signal intensity alterations in cerebellar and brain stem white matter on T1- and T2-weighted images were further characterized regarding their linear dimension and anatomic location. Lateral ventricular size was characterized as a frontal ventricle:brain ratio and as an Evan's Index (Table 2) (20, 21). Third ventricular maximal width was measured in millimeters from axial view images.

The size of the ambient cisterns was characterized as being normal or as showing mild, moderate, or severe enlargement. The anteroposterior and rostral-caudal dimensions of the pons were measured on sagittal view T1-weighted images, with the anteroposterior dimension measured as the greatest perpendicular distance from the ventral surface of the pons to the floor of the fourth ventricle or caudal portion of the sylvian aqueduct. The transverse dimension of the pons was measured on axial view images as its greatest dimension above the middle cerebellar peduncles (MCPs). Because the image data were film based and pooled from multiple imagers, with a lack of identical imaging protocols and with the unavailability to the current investigators of digital image data, a more quantitative characterization or segmentation of areas and volumes of interest could not be achieved.

Statistical Methods

Continuous variables derived from linear measurements of anatomic structures on MR images of symptomatic and control participants were compared by using a two-tailed *t* test for samples of differing size with unequal variances to determine

TABLE 2: Age and MR measurements from symptomatic fragile X premutation carriers and control participants

	Age (yr)	Pons AP (mm)	Pons Trans (mm)	Pons RC (mm)	MCP R (mm)	MCP L (mm)	IV Height (mm)	Ant Horn (mm)	Fr. Cereb-Vent Index	Evan's Index	III Width (mm)
Control participants											
Average	66.1	26	31	29	18	18	11	36	0.32	0.28	6.1
Maximum	76.0	28	33	31	19	22	14	40	0.35	0.31	9.0
Minimum	56.0	23	27	26	15	14	10	31	0.28	0.24	4.0
SD	6.1	1.7	1.7	1.4	1.1	1.9	1.2	2.7	0.02	0.02	1.4
Patients											
Average	67.6	22	25	26	13	13	12	44	0.40	0.35	11.2
Maximum	77.0	24	31	29	17	17	16	60	0.50	0.46	15.0
Minimum	59.0	19	19	23	9	9	8	23	0.30	0.25	7.0
SD	4.7	1.2	2.9	1.8	2.0	2.0	2.5	8.0	0.05	0.05	2.7
P value	0.46	<.005	<.005	<.005	<.005	<.005	0.21	<.005	<.005	<.005	<.005

Note.—AP indicates anteroposterior; Trans, transverse; RC, rostral-caudal; MCP, middle cerebellar peduncle; R, right; L, left; IV Height, vertical dimension of the fourth ventricle measured from the floor of the fourth ventricle to its apex on a midline sagittal image; Ant Horn, maximal width of both anterior horns; Fr. Cereb-Vent Index, ratio of maximal width of both anterior horns to the diameter of inner table of skull along the line of measurement of anterior horn transverse dimension; Evan's index, ratio of maximal width of both anterior horns to the diameter of inner table of skull at its point of greatest transverse diameter on any image; III Width, width of third ventricle; Note that MCP R and MCP L are the narrowest oblique transverse dimension of the right and left middle cerebellar peduncles measured from an axial image. *P* values were derived from Student's *t* test of control versus patient populations.

the probability that there was no difference in the population from which the samples were drawn (Microsoft Excel Statistical Package).

Results

The 17 patients in this study underwent MR imaging at a mean age of 67 years (range, 59–77 years). Before the onset of this neurologic disorder, these persons were healthy and had normal intelligence. Clinical symptoms and physical findings at the time of imaging included intention tremor (89% of the cases), gait ataxia (89%), and dyssynergia (72%). Six patients underwent more detailed neuropsychologic assessment, and all were shown to have executive dysfunction, with cognitive decline in two patients (Table 1). Six patients had impotence. Verbal intelligence quotient was <85 in two of six patients and performance intelligence quotient was <85 in four of six patients who underwent testing. These tests confirmed the cognitive decline described by relatives. Most these patients had college degrees and all were successful in their professional careers. The onset of cognitive symptoms was noted by the patients at a mean age of 60 years. Tremor was noted at a mean age of 58 years (SD of 4 years), and ataxia was noted at a mean age of 62 years (SD of 6 years).

Laboratory findings included the following: CGG repeat lengths clustered in the low to mid premutation range (86 ± 10 CGG repeats). In the six patients for whom FMRP and *FMR1* messenger RNA levels were determined, FMRP levels were in or near the normal range (77 ± 9% FMRP-positive lymphocytes). Messenger RNA levels were elevated in all patients (2.5 ± 0.5-fold elevation).

MR imaging findings were strikingly similar within the patient group, with 15 of 17 showing decreased T1 (Fig 1) and increased T2 signal intensity in deep white matter of the cerebellar hemispheres lateral, inferior, and just superior to the dentate nuclei (Figs 1–4). In 14 of 17, there was a pattern of increased signal intensity on T2-weighted images and sequences extending into the MCPs. This finding was marked (Figs 2–4) or was mild (Fig 1) in prominence. None of the control participants displayed these changes. These findings were consistently symmetrical in their distribution, and in four patients to whom contrast agents were administered, there were no areas of abnormal enhancement (Fig 1). On the diffusion-weighted images that were available for three patients, bilateral regions of increased signal intensity in the MCPs and in deep white matter of the cerebellum lateral, superior, and inferior to the dentate nuclei were shown in only one patient. Quantitative characterization of apparent diffusion coefficients was not available. Signal intensity was normal on the diffusion-weighted images of the other two patients. The dentate and deep cerebellar nuclei were normal in signal intensity on the T1- and T2-weighted images (17 of 17 participants) and on the diffusion-weighted images (three of three participants).

Mild to moderate cerebellar hemisphere cortical volume loss was shown in 15 of 17 study participants (Figs 1–3), with severe cerebellar cortical volume loss in one of 17 (Fig 4). These alterations were manifest on sagittal and axial view T1- and T2-weighted images by prominence in size of sulci and fissures over the cerebellar hemispheres. There were no regions of altered cerebellar cortical T2 signal intensity, and there were no areas of abnormal T1 or T2 signal intensity involving the most lateral aspects of cerebellar white matter. The IV ventricle was normal in height in all 11 patients from whom measurements could be obtained. On axial view images, the MCPs showed decreased oblique transverse dimension (Table 2). In none of the patients was there an alteration in T2 signal intensity or an alteration in contour involving the medulla or the inferior olivary nuclei. Dimensions of the pons were significantly decreased

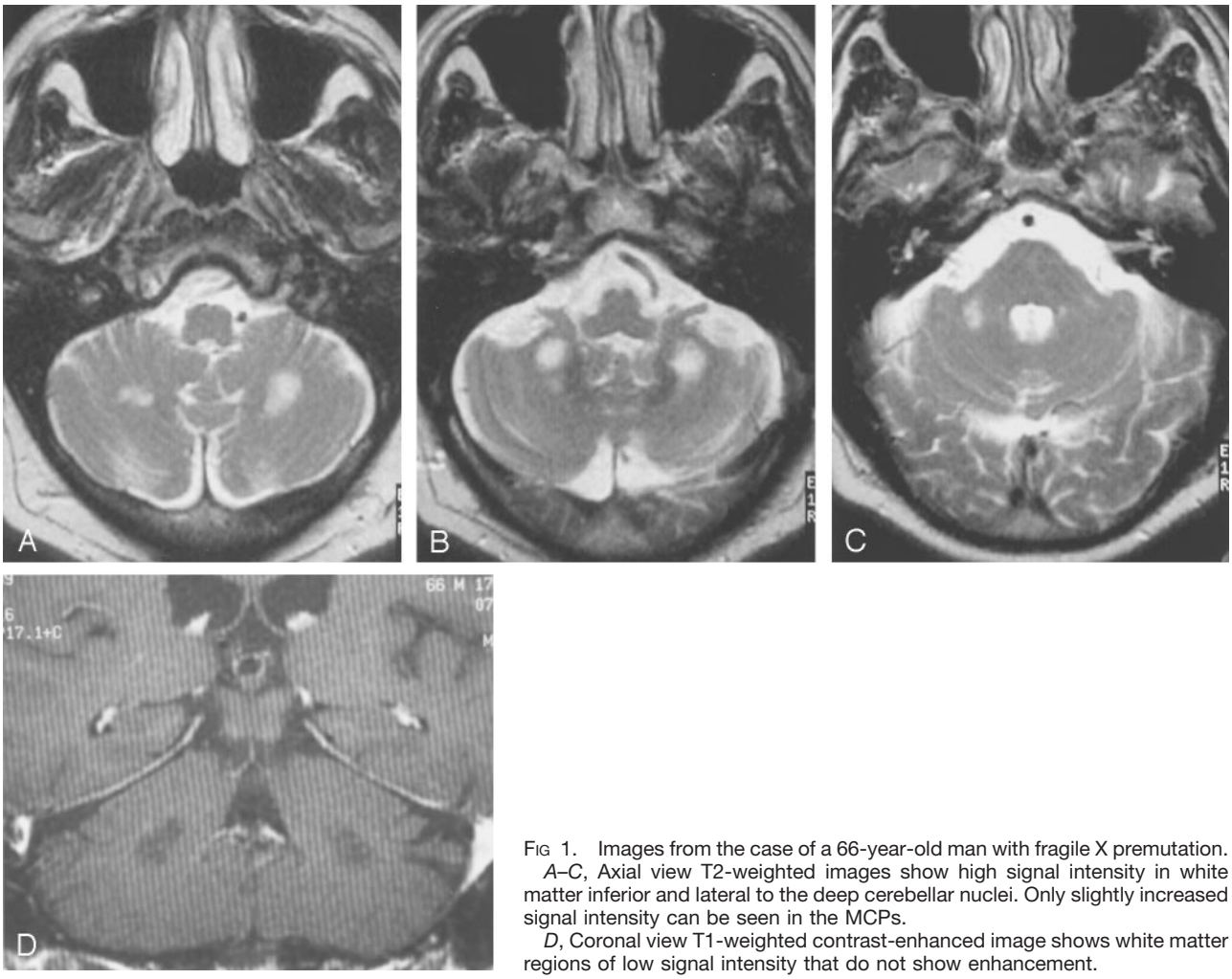

FIG 1. Images from the case of a 66-year-old man with fragile X premutation.
A–C, Axial view T2-weighted images show high signal intensity in white matter inferior and lateral to the deep cerebellar nuclei. Only slightly increased signal intensity can be seen in the MCPs.
D, Coronal view T1-weighted contrast-enhanced image shows white matter regions of low signal intensity that do not show enhancement.

when compared with those of control participants (Table 2).

A pattern of mild (three of 17 patients), moderate (10 of 17 patients) (Fig 3), or severe (four of 17 patients) (Figs 2 and 4) cortical volume loss was shown over the frontal lobes, with mild (four of 17 patients), moderate (nine of 17 patients), or severe (four of 17 patients) cortical volume loss also shown to involve parietal cortex in the premutation carriers. Mild temporal cortical volume loss occurred in six of 17 patients and moderate temporal cortical volume loss in eight of 17 patients (Fig 3). No areas of apparent cerebral cortical infarction and no areas of significant subcortical increased T2 signal intensity were observed. Areas of subependymal and deep white matter increased T2 signal intensity, disproportionate for age, were shown in the frontal lobe in 14 of 17 patients and in the parietal lobes in 13 of 17 patients (Figs 3 and 4). The size of the hippocampal gyri could not be quantitatively characterized on images available for this study. Evan's Index averaged 0.35 (range, 0.25–0.46) in the patient group and 0.28 (range, 0.24–0.31) in the control group ($P < .005$) (Table 2). The frontal cerebro-ventricular index averaged 0.40 (range, 0.30–0.50) in the patient group and 0.32 (range, 0.28–0.35) in the control group ($P < .005$). The mean width of the third ventricle was widened (11 mm) when compared with that of the control participants (6 mm, $P < .01$) (Table 2). There were no regions of altered T1 or T2 signal intensity involving the caudate nucleus, globus pallidus, or putamen. The thalamic nuclei showed no areas of altered T1 or T2 signal intensity. There was mild to moderate enlargement of the ambient cisterns in 15 of 15 patients (Fig 3), with no associated alteration in T2 signal intensity of the mesencephalon or rostral pons. The transverse dimension of the mesencephalon was decreased by perceptual characterization in 16 of 17 patients (Fig 3), and the ambient cistern was widened on the axial view images of 17 of 17 patients. The corpus callosum showed a mild or moderate decreased thickness at the midline in 14 of 16 patients (Figs 2 and 4).

Discussion

Fragile X syndrome is caused by an absence or deficiency of FMRP, a protein that is important for early brain development, for the translation of other messages important for synaptic structure development, and for brain maturation and plasticity. Although the focus of fragile X syndrome has been on

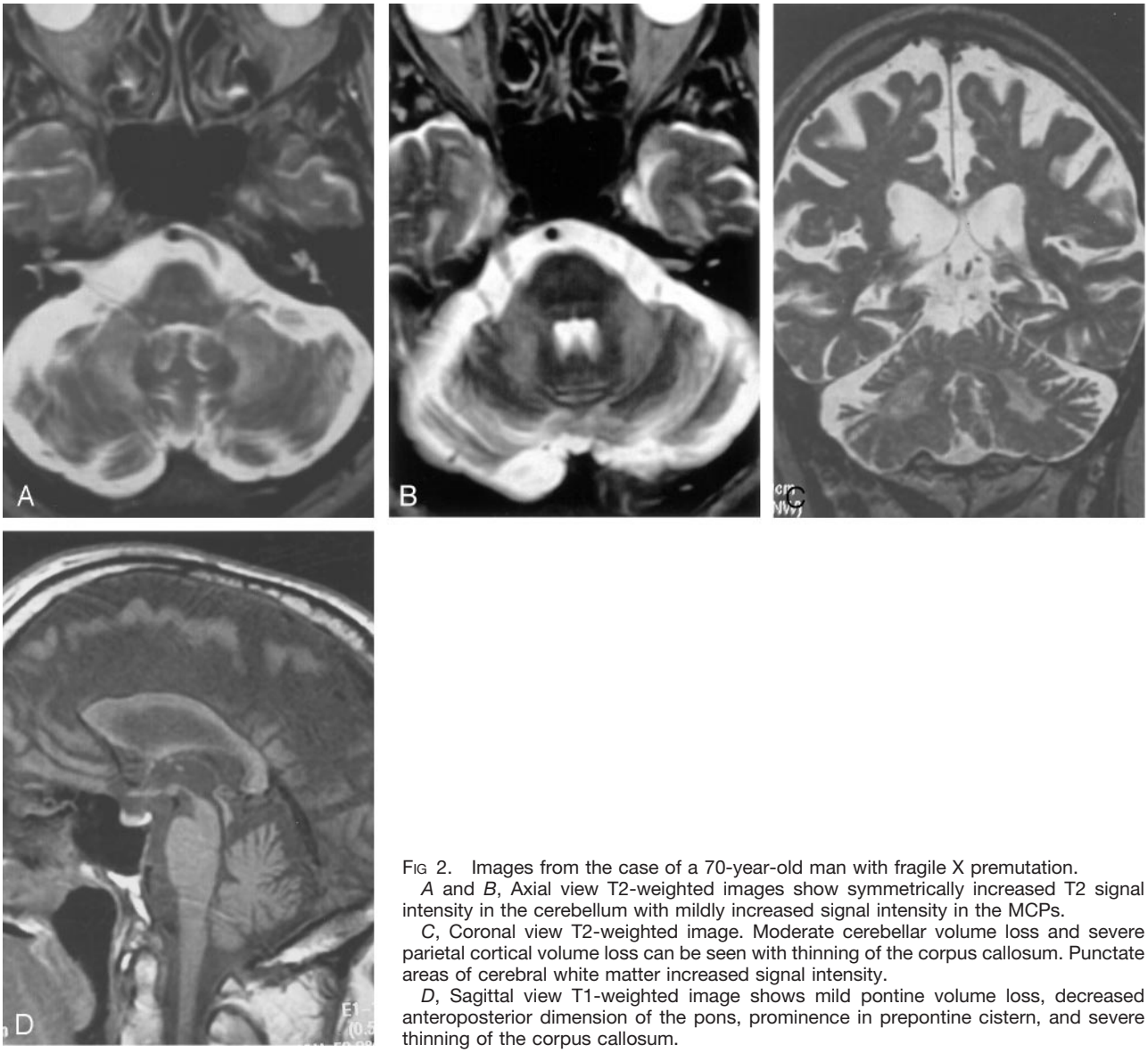

FIG 2. Images from the case of a 70-year-old man with fragile X premutation.

A and *B*, Axial view T2-weighted images show symmetrically increased T2 signal intensity in the cerebellum with mildly increased signal intensity in the MCPs.

C, Coronal view T2-weighted image. Moderate cerebellar volume loss and severe parietal cortical volume loss can be seen with thinning of the corpus callosum. Punctate areas of cerebral white matter increased signal intensity.

D, Sagittal view T1-weighted image shows mild pontine volume loss, decreased anteroposterior dimension of the pons, prominence in prepontine cistern, and severe thinning of the corpus callosum.

its relationship to early child development, a newly recognized disorder, associated with fragile X premutation, has been noted to manifest in elderly men as the presence of tremor, ataxia, dyssynergia, cognitive decline, rigidity, and impotence. MR imaging findings for this group of patients have striking uniformity, with 15 of 17 patients showing decreased T1 and increased T2 signal intensity in the deep white matter of the cerebellar hemispheres lateral, inferior, and just superior to the dentate nuclei. In 14 of 17 patients, similar changes were shown in the MCPs. Cerebral and cerebellar cortical volume loss, volume loss of the mesencephalon and pons, and loss in the cross-sectional area of the corpus callosum, all disproportionate for age, are additional findings that seem to be typical. The diagnosis of fragile X premutation is of importance because this disorder may be a significant cause of progressive "sporadic" spinocerebellar degeneration of late onset. Although the diagnosis of fragile X premutation disorder can be suspected on the basis of symptoms, imaging findings, and/or a family history that includes an established diagnosis of fragile X syndrome, definitive genetic testing is necessary for diagnosis. The recognition of this disorder among adult patients presenting with appropriate clinical and imaging findings may also have a significant effect on family planning among the children of patients with this diagnosis.

Neurohistologic studies of the brains of four elderly male fragile X premutation carriers have shown Bergman gliosis and Purkinje cell loss with proximal axonal swelling indicative of degeneration in remaining Purkinje cells (12). In one case, spongiosis was noted in cerebellar white matter. Eosinophilic ubiquitin-positive intranuclear inclusions were shown in neuronal and astrocytic nuclei of the cerebrum and brain stem, with inclusions being most numerous in the hippocampal gyri. Neurons of the dentate nuclei contained the intranuclear inclusions, although Purkinje cells did not. The relationship between MR imaging

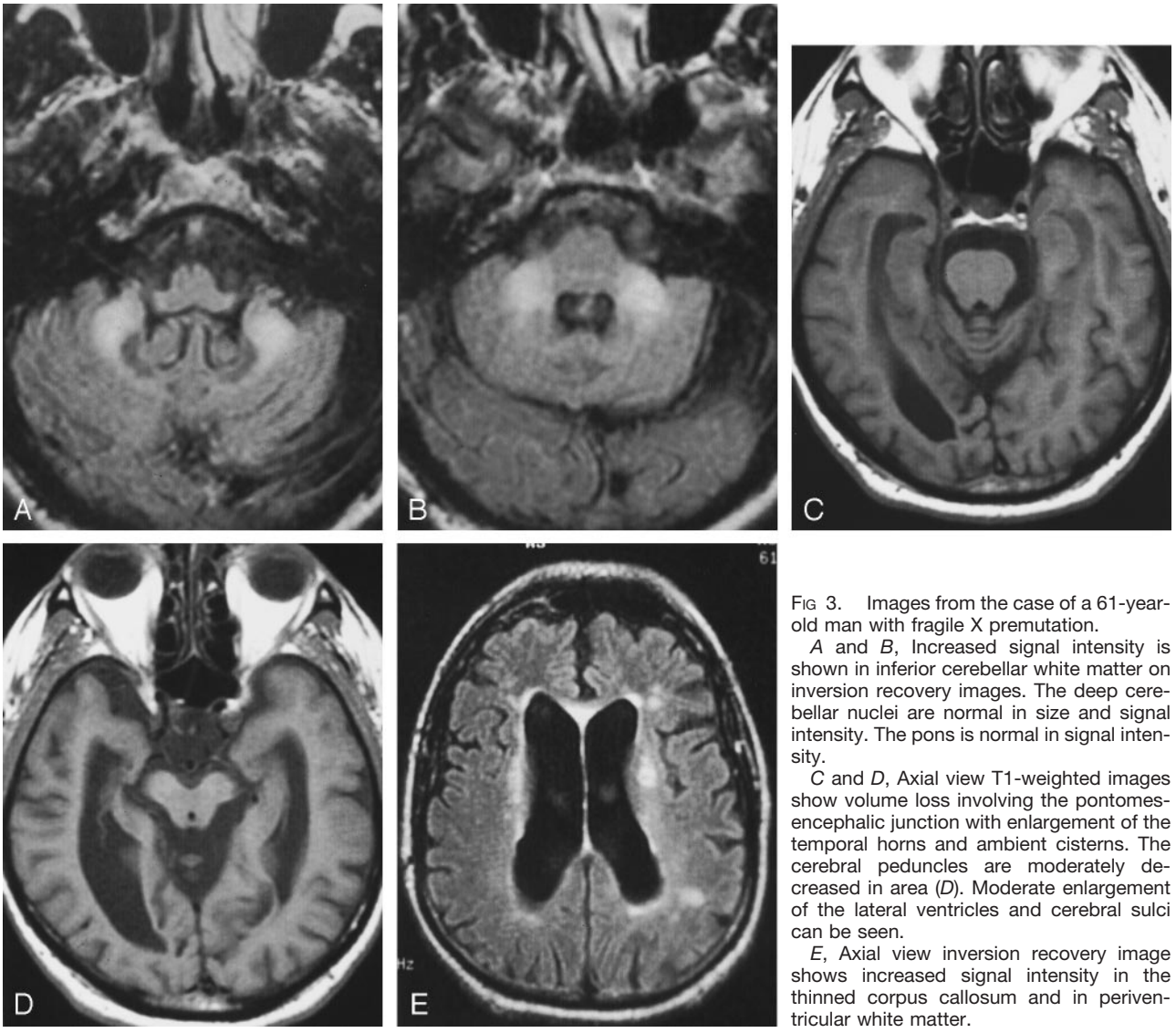

FIG 3. Images from the case of a 61-year-old man with fragile X premutation.

A and *B*, Increased signal intensity is shown in inferior cerebellar white matter on inversion recovery images. The deep cerebellar nuclei are normal in size and signal intensity. The pons is normal in signal intensity.

C and *D*, Axial view T1-weighted images show volume loss involving the pontomesencephalic junction with enlargement of the temporal horns and ambient cisterns. The cerebral peduncles are moderately decreased in area (*D*). Moderate enlargement of the lateral ventricles and cerebral sulci can be seen.

E, Axial view inversion recovery image shows increased signal intensity in the thinned corpus callosum and in periventricular white matter.

findings shown for the 17 premutation patients included in this study and the description of intranuclear inclusions, Purkinje cell loss, gliosis, and spongiosis involving cerebellar white matter remains to be determined. MR images of these four patients were not available.

Laboratory findings for the participants of the current study were remarkable in three respects. First, CGG repeat lengths were in the low to mid premutation range, with a mean of 86 CGG repeats. Although this distribution probably reflects the preponderance of smaller alleles in the premutation population, it does indicate that clinical involvement begins in the low premutation range. Second, FMRP levels were in or near the normal range, with a mean of 78% for the fraction of FMRP(+) lymphocytes. This suggests that the MR imaging findings are unlikely to be a direct consequence of a protein deficit or that brain atrophy or white matter disease can occur with only mild deficits of FMRP levels. Finally, *FMR1* messenger RNA levels were elevated in all participants, with a mean 2.5-fold elevation. This is the most consistent laboratory finding within the current group of premutation male patients, and it may be related to the MR imaging findings reported herein.

In 1991, the gene responsible for fragile X syndrome was found to contain an unstable, expanded $(CGG)_n$ trinucleotide repeat in its 5′ untranslated region (22). Since then, the expansion of unstable trinucleotide repeats has become a novel genetic paradigm. To date, 15 trinucleotide repeat expansion disorders have been reported. These disorders can be divided into two groups: those with coding and those with noncoding repeats. The coding repeat disorders are Kennedy disease, Huntington disease, spinocerebellar ataxia types 1, 2, 3, 6, and 7, and Dentatorubral-Pallidoluysian atrophy. These disorders are all caused by exonic CAG repeats that are translated to a long polyglutamine tract conferring a gain of function. Midlife onset of symptomatic neurodegeneration is characteristic. Nuclear inclusions are also a hallmark of these polyglutamine disorders. The noncoding repeat diseases are fragile X and fragile XE $(CGG)_n$ syndrome, myotonic dystrophy $(CTG)_n$, Friedreich ataxia $(GAA)_n$, and spinocerebellar ataxia types 8

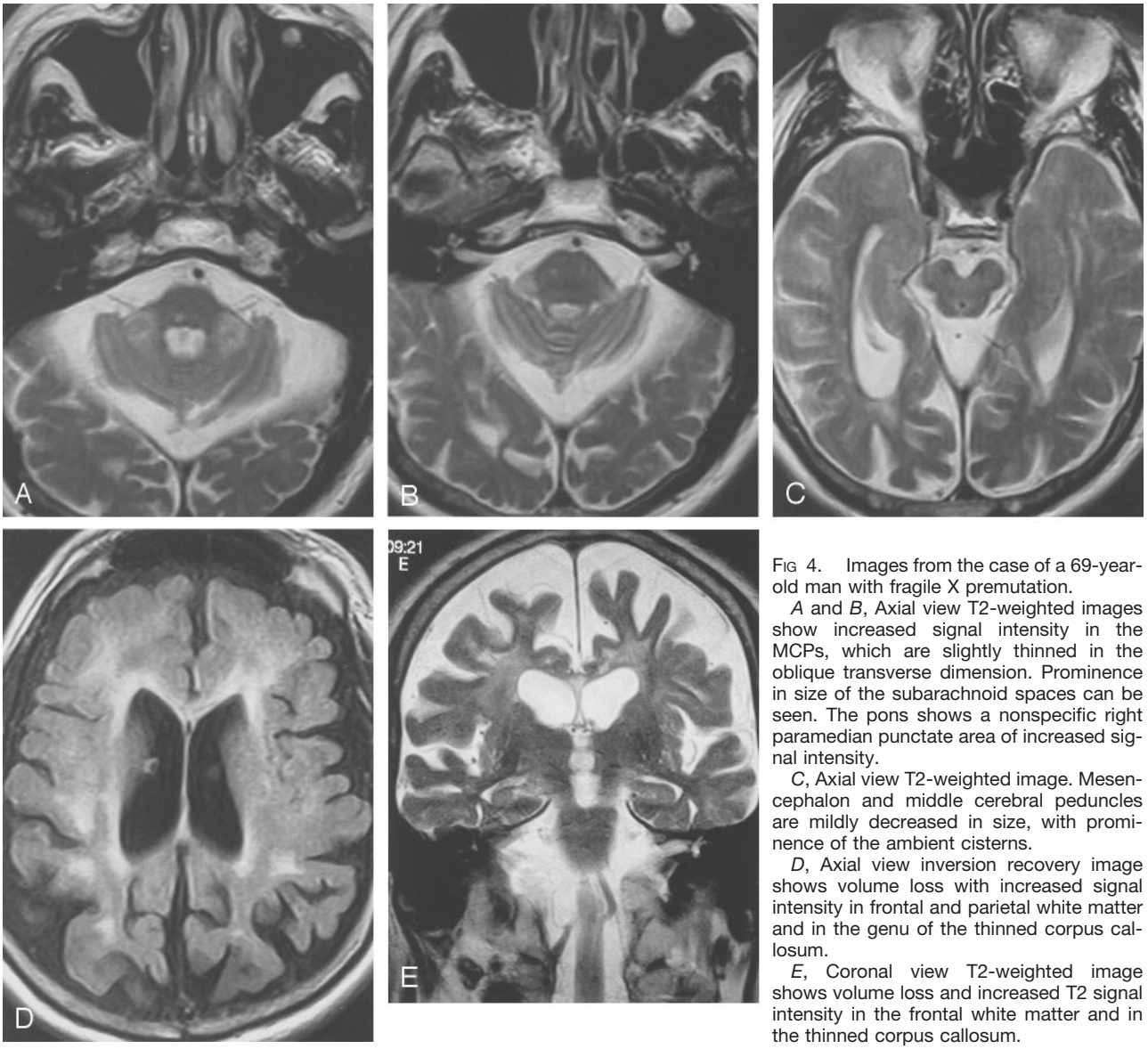

FIG 4. Images from the case of a 69-year-old man with fragile X premutation.

A and *B*, Axial view T2-weighted images show increased signal intensity in the MCPs, which are slightly thinned in the oblique transverse dimension. Prominence in size of the subarachnoid spaces can be seen. The pons shows a nonspecific right paramedian punctate area of increased signal intensity.

C, Axial view T2-weighted image. Mesencephalon and middle cerebral peduncles are mildly decreased in size, with prominence of the ambient cisterns.

D, Axial view inversion recovery image shows volume loss with increased signal intensity in frontal and parietal white matter and in the genu of the thinned corpus callosum.

E, Coronal view T2-weighted image shows volume loss and increased T2 signal intensity in the frontal white matter and in the thinned corpus callosum.

$(CTG)_n$ and 12 $(CAG)_n$. The phenotypes in these latter disorders may be a consequence of the loss of function of the respective protein but also may be related to altered RNA level or function. These diseases are typically multisystem disorders involving dysfunction/degeneration that involves many different tissues.

Achieving a specific diagnosis among adult patients with late onset spinocerebellar degeneration is difficult. The challenge relates to the complex nosology and symptomatology of disorders with adult onset ataxia, to the absence of definitive laboratory markers for many specific diseases causing these symptoms, and to the relative lack of definitive imaging findings to correlate with specific diagnoses. The recent correlation of the fragile X premutation abnormality with late adult onset of intention tremor, ataxia, autonomic dysfunction, rigidity, and cognitive decline now indicates an additional diagnosis to consider during the evaluation of patients with symptoms of spinocerebellar degeneration (11).

Although the MR imaging findings of symmetrically increased T2 signal intensity within the MCPs and adjacent cerebellar white matter have been shown in this study to be characteristic of symptomatic elderly men with fragile X premutation, these findings are not specific. A differential diagnosis needs to be considered. One such diagnostic consideration is a disorder recently reported in three young adult siblings who developed progressive ataxia, dysarthria, nystagmus, mild cognitive impairment, and sensorimotor neuropathy (23). MR imaging of two siblings showed symmetrically increased T2 signal intensity in the MCPs and adjacent cerebellar white matter and symmetrically increased T2 signal intensity in the thalamic nuclei. Increased T2 signal intensity was seen in the inferior olivary nuclei. Mild cerebral and cerebellar cortical volume loss was observed. The MR imaging findings in the brain stem and cerebellum of these kindred are similar to those in the fragile X premutation cases that we report herein. An important distinction is that none of the fragile X

premutation participants showed the altered thalamic T2 signal intensity that was characteristic of these kindred.

Olivopontocerebellar atrophy is an additional disorder with occasional increased T2 signal intensity in the MCPs and in deep cerebellar white matter adjacent to the dentate nuclei (24–26). The term *olivopontocerebellar atrophy* is a collective one, used to describe a number of progressive neurologic disorders, all of which have in common the occurrence of neuronal degeneration and gliosis involving the inferior olives, pons, and cerebellum (27). These disorders can be divided into two general types. The first is familial or inherited, and the second is sporadic. Sporadic olivopontocerebellar atrophy is frequently a precursor to multiple system atrophy in which glial cells are shown to have cytoplasmic inclusions (27). Glial cytoplasmic inclusions are rare in familial olivopontocerebellar atrophy (27). Autopsy studies of cases of sporadic olivopontocerebellar atrophy have shown gliosis and loss of transverse fiber tracts in the pons, MCP, and cerebellum. Transverse pontine fibers fail to stain for myelin, and Purkinje cell loss occurs (24). MR imaging reveals atrophy of the pons, especially its ventral and inferior portion, with volume loss of the cerebellum and MCP (24). Symmetrically increased signal intensity frequently occurs on spin diffusion- and T2-weighted images involving the transverse pontine fibers and involving the MCPs and adjacent white matter of the cerebellum (24, 26). Changes in the signal intensity of transverse pontine fibers were seen on the spin diffusion-weighted images of only one fragile X premutation participant at 1.5 T and on none at low field strength. None of our participants had alterations in the central pons shown by T2-weighted imaging. As with the fragile X premutation carriers, most patients with sporadic olivopontocerebellar atrophy have evidence of cerebral cortical volume loss and no alteration in T2 signal intensity of the striatum (24).

Increased T2 signal intensity in the MCPs and adjacent deep cerebellar white matter has uncommonly been shown in patients with various specific forms of autosomal dominant cerebellar ataxia. Autosomal dominant cerebellar ataxia is divided into clinical types I, II, III, and IV depending on the presence of cerebellar symptoms combined with the occurrence of pyramidal, extrapyramidal, or cognitive dysfunction (type I); cerebellar symptoms combined with pigmentary maculopathy (type II); pure cerebellar symptoms without or with mild pyramidal symptoms (type III); and cerebellar symptoms combined with myoclonus (type IV). Each clinical autosomal dominant cerebellar ataxia type has now been recognized to contain several specific types of spinocerebellar atrophy, most of which have been identified on the basis of specific genetic alterations. Spinocerebellar ataxia type 6 with clinical symptoms of an autosomal dominant cerebellar ataxia type III has been described as occurring in a single patient in association with increased T2 signal intensity in the MCPs and mild atrophy of the pons and cerebellum (28). Three separately reported cases of spinocerebellar ataxia type 6 have not had the alteration in posterior fossa white matter T2 signal intensity (29). Patients with spinocerebellar ataxia types 1, 2, 3, 5, 8, 12, and 13 have been shown to have volume loss of varying severity involving the cerebellar hemispheres, vermis, and pons (28–37).

Dentatorubral-Pallidoluysian atrophy is an autosomal dominant spinocerebellar degeneration associated with increased CAG repeats in chromosome 12p. It presents as a juvenile form that is manifest by ataxia, dementia, and seizures that are predominately myoclonic. It also presents as early or late adult forms with ataxia and combinations of dementia, choreoathetosis, or seizures. MR imaging has revealed volume loss that involves the cerebellum, brain stem, and cerebral cortex (38–40). Increased T2 signal intensity involving the white matter of the central pons, the mesencephalon, the thalamic nuclei, and the cerebral hemispheres can be seen. The age at onset of symptomatology and the distribution of the T2 abnormality suggests that the development of imaging alterations occurs in a caudal to rostral manner. Increased cerebellar white matter and MCPs T2 signal intensity has not been characteristic of Dentatorubral-Pallidoluysian atrophy.

Multiple system atrophy is an additional spinocerebellar degeneration that has been associated with increased T2 signal intensity in the MCPs and in adjacent deep white matter of the cerebellum (41). Multiple system atrophy, one of the more common sporadic adult neurodegenerative disorders, is manifest by a variable combination of extrapyramidal, cerebellar, and autonomic dysfunction. Although glial cytoplasmic inclusions have been shown, there are no specific biochemical markers and diagnosis is based predominately on clinical findings. Included under the heading of multiple system atrophy are striatonigral degeneration, the Shy-Drager syndrome, and cases of sporadic olivopontocerebellar atrophy that are associated with autonomic dysfunction or extrapyramidal symptomatology. MR imaging in cases of multiple system atrophy is characterized by pontine volume loss with a distinctive late caudal tapering of the anterior contour of the pons on sagittal images. There is eventual prominent narrowing of the oblique transverse dimension of the MCPs on axial view images and enlargement of the fourth ventricle. Findings of low T2 signal intensity in the putamen have been shown in a significant number of patients (41, 42), as has a thin margin of high T2 signal intensity at the lateral aspect of the putamen (42). Dimensions of the mesencephalon are reduced, and there is moderate to severe cerebellar hemisphere volume loss. Regions of increased T2 signal intensity in cerebellar deep white matter surrounding the dentate nuclei and in the MCPs are reported with lower frequency (41, 42), and they are generally less prominent in severity than the alterations shown in this group of symptomatic fragile X premutation carriers. The degree of pontine volume loss was less severe in this group of symptomatic patients with the fragile X premutation than has been reported in association with multiple system atrophy.

Wilson's disease has been described as having increased T2 signal intensity in the deep white matter of the cerebellar hemispheres adjacent to the dentate nuclei (43). We have seen such alteration extending into the MCPs of patients with Wilson's disease. This finding generally occurs later in the disease process, and it has, in our own experience, invariably been associated with a symmetric decrease in volume and with increased or mixed increased and decreased T2 signal intensity involving the putamen. The occurrence of symmetrically increased T2 signal intensity in the MCPs and deep white matter of the cerebellum with sparing of the dentate nuclei, similar to the findings seen in the current series of patients, has also been described as occurring in a single patient with acquired non-Wilsonian hepatocerebral degeneration (44).

Infarction in the distribution of the anterior inferior cerebellar arteries caused by vertebral artery dissection has been associated with bilateral increased T2 signal intensity in the MCPs (45). The abrupt onset of symptomatology should clinically distinguish vascular cause from the disorders described above. Spongiform dysplastic changes associated with increased T2 signal intensity have also been described as occurring in the peridentate white matter of the cerebellum and MCPs in patients with neurofibromatosis (46). Finally, in patients with progressive supranuclear palsy, increased signal intensity has been described as occurring in the superior cerebellar peduncles on proton diffusion-weighted images (47), although normal signal intensity can be seen in the deep cerebellar white matter and MCPs. Alterations involving the superior cerebellar peduncles were not shown to occur in the patients included in the current study.

Conclusion

The development of progressive intention tremor, ataxia, rigidity, and occasional cognitive decline has been shown to be associated with a characteristic MR imaging pattern among elderly male patients with fragile X premutation. This pattern includes increased T2 signal intensity in the MCPs and deep white matter of the cerebellum that is medial, superior, and inferior to the dentate nuclei. Additional findings include volume loss involving the pons, mesencephalon, cerebellar cortex, cerebral cortex, white matter of the cerebral hemispheres, and corpus callosum. Patchy and confluent regions of increased T2 signal intensity are also much more prominent in periventricular and deep white matter of the cerebral hemispheres and in the corpus callosum than in control participants. These findings, although not specific, can lead to consideration of a diagnosis of the fragile X premutation that may have significant implications for its potential occurrence in the children of reproductive age female relatives of the identified patient. Fragile X syndrome is the most common genetic cause of mental retardation. Definitive diagnosis of the fragile X premutation requires genetic testing. It is important to recognize that not all persons with the premutation develop the tremor/ataxia syndrome that prompted imaging in the current series of patients. The frequency of this syndrome among patients with adult onset ataxia, late onset intention tremor, or extrapyramidal symptomatologies remains to be determined, as do the full clinical and imaging dimensions of the fragile X premutation syndrome.

Acknowledgments

This research was supported in part by National Institute of Child Health & Human Development grant HD36071 and by the M.I.N.D. Institute.

References

1. Rousseau F, Rouillard P, Morel ML, Khandjian EW, Morgan K. **Prevalence of carriers of premutation-size alleles of the FMRI gene and implications for the population genetics of the fragile X syndrome.** *Am J Hum Genet* 1995;57:1006–1018
2. Rousseau F, Morel M-L, Rouillard P, Khandjian EW, Morgan K. **Surprisingly low prevalence of FMR1 premutation among males from the general population.** American Society of Human Genetics Annual Meeting, October 28–November 1, 1997, Baltimore.
3. Hagerman RJ, Hagerman PJ. **Fragile X syndrome: a model of gene-brain-behavior relationships.** *Mol Genet Metab* 2001;74:89–97
4. Dorn MB, Mazzocco MM, Hagerman RJ. **Behavioral and psychiatric disorders in adult male carriers of fragile X.** *J Am Acad Child Adolesc Psychiatry* 1994;256–264
5. Franke P, Leboyer M, Gansicke M, et al. **Genotype-phenotype relationship in female carriers of the premutation and full mutation of FMR-1.** *Psych Res* 1998;80:113–127
6. Sobesky WE, Hagerman RJ, Cronister A, eds. *The Treatment of Emotional and Behavioral Problems in Fragile X Syndrome: Diagnosis, Treatment, and Research.* 2nd ed. Baltimore: The Johns Hopkins University Press; 1996:332–348
7. Franke P, Maier W, Hautzinger M, et al. **Fragile-X carrier females: evidence for a distinct psychopathological phenotype.** *Am J Med Genet* 1996;64:334–339
8. Riddle JE, Cheema A, Sobesky WE, et al. **Phenotypic involvement in females with the FMR1 gene mutation.** *Am J Ment Retard* 1998; 102:590–601
9. Schwartz CE, Dean J, Howard Peebles PN, et al. **Obstetrical and gynecological complications in fragile X carriers: a multicenter study.** *Am J Med Genet* 1994;51:400–402
10. Allingham-Hawkins DJ, Babul-Hirji R, Chitayat D, et al. **Fragile X premutation is a significant risk factor for premature ovarian failure: The International Collaborative POF in Fragile X Study: preliminary data.** *Am J Med Genet* 1999; 83:322–325
11. Hagerman RJ, Leehey M, Heinrichs W, et al. **Intention tremor, parkinsonism and generalized brain atrophy in older male carriers of fragile X.** *Neurology* 2001;57:127–130
12. Greco CM, Hagerman RJ, Tassone F, et al. **Neuronal intranuclear inclusions in a new cerebellar tremor/ataxia syndrome among fragile X carriers.** *Brain* 2002;125:1760–1771
13. Hagerman RJ, Greco CM, Chudley AE, et al. **Neuropathology and neurodegenerative features in some older male premutation carriers of fragile X syndrome.** *Am J Hum Genet* 2001;69[suppl]:177
14. Taylor AK, Safanda JF, Fall MZ, et al. **Molecular predictors of cognitive involvement in female carriers of fragile X syndrome.** *JAMA* 1994;271:507–514
15. Tassone F, Hagerman RJ, Taylor AK, Hagerman PJ. **A majority of fragile X males with methylated, full mutation alleles have significant levels of FMR1 messenger RNA.** *J Med Genet* 2001;38:453–456
16. Tassone F, Hagerman RJ, Taylor AK, Gane LW, Godfrey TE, Hagerman PJ. **Elevated levels of FMR1 messenger RNA in g carrier males: a new mechanism of involvement in the fragile X syndrome.** *Am J Hum Genet* 2000;66:6–15
17. Willemsen R, Mohkamsing S, de Vries BB, et al. **Rapid antibody test for fragile X syndrome.** *Lancet* 1995;345:1147–1148
18. Willemsen R, Smits A, Mohkamsing S, et al. **Rapid antibody test for diagnosing fragile X syndrome: a validation of the technique.** *Hum Genet* 1997;99:308–311

19. Tassone F, Hagerman RJ, Ilke DN, et al. **FMRP expression as a potential prognostic indicator in fragile X syndrome.** *Am J Med Genet* 1999;84:250–261
20. Synek V, Reuben JR, Du Boulay GH. **Comparing Evans' index and computerized axial tomography in assessing relationship of ventricular size to brain size.** *Neurology* 1976;26:231–233
21. Hahn FJ, Rim K. **Frontal ventricular dimensions on normal computed tomography.** *Radiology* 1976;126:593–596
22. Oberle I, Rousseau F, Heitz D, et al. **Instability of a 550-base pair DNA segment and abnormal methylation in fragile X syndrome.** *Science* 1991;252:1097–1102
23. Rantamaki M, Krahe R, Paetau A, Cormand B, Mononen I, Udd B. **Adult-onset autosomal recessive ataxia with thalamic lesions in a Finnish family.** *Neurology* 2001;57:1043–1049
24. Savoiardo M, Strada L, Girotti F, et al. **Olivopontocerebellar atrophy: MR diagnosis and relationship to multisystem atrophy.** *Radiology* 1990;174:693–696
25. Gilman S, Little R, Johanns J, et al. **Evolution of sporadic olivopontocerebellar atrophy into multiple system atrophy.** *Neurology* 2000; 55:527–532
26. Adachi M, Hosoya T, Yamaguchi K, Kawanami T, Kato T. **Diffusion- and T2-weighted MRI of the transverse pontine fibres in spinocerebella degeneration.** *Neuroradiology* 2000;42:803–809
27. Caraceni T, Savoiardo M, Grisoli M, Testa D, Girotti F. **Multiple system atrophy.** *Arch Neurol* 1996;53:212–213
28. Nakagawa N, Katayama T, Makita Y, Kuroda K, Aizawa H, Kikuchi K. **A case of spinocerebellar ataxia type 6 mimicking olivopontocerebellar atrophy.** *Neuroradiology* 1999;41:505–503
29. Satoh JI, Tokumoto H, Yukitake M, et al. **Spinocerebellar ataxia type 6: MRI of three Japanese patients.** *Neuroradiology* 1998;40: 222–227
30. Namekawa M, Takiyama Y, Ando Y, et al. **Choreiform movements in spinocerebellar ataxia type 1.** *J Neurol Sci* 2001;187:103–106
31. Nakayama T, Nakayama K, Takahashi Y, et al**. Case of spinocerebellar ataxia type 1 showing high intensity lesions in the frontal white matter on T2-weighted magnetic resonance images.** *Med Sci Monit* 2001;72:299–303
32. Klockgether T, Skalej M, Wedekind D, et al. **Autosomal dominant cerebella ataxia type I MRI-based volumetry of posterior fossa structures and basal ganglia in spinocerebellar ataxia types 1, 2 and 3.** *Brain* 1998;121:1687–1693
33. O'Hearn E, Holmes SE, Calvert PC, Ross CA, Margolis RL. **SCA-12: tremor with cerebellar and cortical atrophy is associated with a CAG repeat expansion.** *Neurology* 2001;56;299–303
34. Day JW, Schut LJ, Moseley ML, Durand AC, Ranum LP. **Spinocerebellar ataxia type 8.** *Neurology* 2000;55:649–657
35. Ikeda Y, Shizuka-Ikeda M, Watanabe M, Schmitt M, Okamoto K, Shoji M. **Asymptomatic CTG expansion at the SCA8 locus is associated with cerebellar atrophy on MRI.** *J Neurol Sci* 2000:182:76–79
36. Stevanin G, Herman A, Brice A, Dürr A. **Clinical and MRI findings in spino-cerebellar ataxia type 5.** *Neurology* 1999;53;355–1357
37. Giuffrida S, Saponara R, Restivo D, et al. **Supratentorial atrophy in spinocerebellar ataxia type 2: MRI study of 20 patients.** *J Neurol* 1999;246:383–388
38. Tomiyasu H, Yoshii F, Ohnuki Y, Ikeda JE, Shinohara. **The brainstem and thalamic lesions in dentatorubral-pallidoluysian atrophy: an MRI study.** *Neurology* 1998;50:1887–1890
39. Miyazaki M, Kato T, Hashimoto T, Harada M, Kondo I, Kuroda Y. **MR of childhood-onset dentatorubral-pallidoluysian atrophy.** *AJNR Am J Neuroradiol* 1995;16:1834–1836
40. Koide R, Onodera O, Ikeuchi T, et al. **Atrophy of the cerebellum and brainstem in dentatorubral pallidoluysian atrophy: influence of CAG repeat size on MRI findings.** *Neurology* 1997;49:1605–1612
41. Schulz JB, Klockgether T, Petersen D, et al. **Multiple system atrophy: natural history, MRI morphology and dopamine receptor imaging with ^{123}IBZM-SPECT.** *J Neurol Neurosurg Psychiatry* 1994; 57:1047–1056
42. Bhattacharya K, Saadia D, Eisenkraft B, et al. **Brain magnetic resonance imaging in multiple-system atrophy and Parkinson disease: a diagnostic algorithm**. *Arch Neurol* 2002;59:835–842
43. Matsuura T, Sasaki H, Tashiro K. **Atypical MR findings in Wilson's disease: pronounced lesions in the dentate nucleus causing tremor.** *J Neurol Neurosurg Psychiatry* 1998;64:161
44. Lee J, Lacomis D, Comu S, Jacobson J, Kanal E**. Acquired hepatocerebral degeneration: MR and pathologic findings.** *AJNR Am J Neuroradiol* 1998;19:485–487
45. Akiyama K, Takizawa S, Tokuoka K, Ohnuki Y, Kobayashi N, Shinohara Y. **Bilateral middle cerebellar peduncle infarction caused by traumatic vertebral artery dissection.** *Neurology* 2000;56: 693–695
46. Menor F, Marti-Bonmati L, Arana E, Poyatos C, Cortina H. **Neurofibromatosis type 1 in children: MR imaging and follow-up studies of central nervous system findings.** *Eur J Radiol* 1998;26:121–131
47. Oka M, Katayama S, Imon Y, Ohshita T, Mimori Y, Nakamura S. **Abnormal signals in proton density-weighted MRI of the superior cerebellar peduncle in progressive supranuclear palsy.** *Acta Neurol Scand* 2001;104:1–5